Data in Brief 30 (2020) 105649

Contents lists available at ScienceDirect

Data in Brief

journal homepage: www.elsevier.com/locate/dib

Data Article

Mitochondrial lipid profiling data of a traumatic optic neuropathy model

Ronaldo Nuesi [1,2], Ryan A. Gallo [1], Sean D. Meehan [1], John V. Nahas [1], Galina Dvoriantchikova [1], Daniel Pelaez [1,*], Sanjoy K. Bhattacharya [1,*]

[1] *Department of Ophthalmology, Bascom Palmer Eye Institute, University of Miami Miller School of Medicine, Miami, FL 33136, USA*
[2] *Herbert Wertheim College of Medicine, Florida International University, Miami, FL 33199, USA*

ARTICLE INFO

Article history:
Received 2 April 2020
Revised 21 April 2020
Accepted 23 April 2020
Available online 30 April 2020

Keywords:
Traumatic Optic Neuropathy
Neurodegeneration
Mitochondrial lipids
Liquid Chromatography-Mass Spectrometry
Lipidomics
Metabolomics

ABSTRACT

Traumatic optic neuropathy (TON) is a degenerative process that occurs in a subset of patients following blunt force trauma to the head. This condition is characterized by retinal ganglion cell (RGC) death and axon degeneration within the optic nerve [1]. At the cellular level, mitochondrial changes are associated with many optic neuropathies [2, 3]. Here, we provide a dataset demonstrating changes in the optic nerve mitochondrial lipid profile of a sonication-induced traumatic optic neuropathy (SI-TON) mouse model at 1, 7, and 14 days after injury. 32 C57BL/6J mice were separated into 4 groups (control, 1, 7, and 14 days) of 8, with 4 males and 4 females in each. Mice were exposed to sonication-induced trauma as described previously (by Tao et al) and optic nerves were harvested at 1, 7, or 14 days following injury [4]. Mitochondria were isolated from homogenized optic nerves and lipids were extracted. Extracted mitochondrial lipids were analysed with a Q-Exactive Orbitrap Liquid Chromatography-Mass Spectrometer (LC MS-MS). Further analysis of raw data was conducted with LipidSearch 4.1.3 and Metaboanalyst 4.0. This data is publicly available at the Metabolomics Workbench, http://www.metabolomicsworkbench.org (Project ID: PR000905).

* Corresponding authors.
E-mail addresses: dpelaez@med.miami.edu (D. Pelaez), SBhattacharya@med.miami.edu (S.K. Bhattacharya).

https://doi.org/10.1016/j.dib.2020.105649

Specifications Table

Subject	Cell Biology
Specific subject area	Mitochondria, Lipids
Type of data	Table Figure
How data were acquired	Liquid Chromatography Q-Exactive Orbitrap Mass Spectrometry, LipidSearch 4.1.3, Metaboanalyst 4.0
Data format	Raw Analyzed Filtered
Parameters for data collection	Optic nerve, age, survival
Description of data collection	Sonication-induced trauma to optic nerves, optic nerves collected and mitochondria isolated. Mitochondrial lipids extracted with butanol-methanol method and analysed with mass spectrometry, further analysed with Metaboanalyst 4.0 and LipidSearch 4.1.3
Data source location	Bascom Palmer Eye Institute, Miller School of Medicine at University of Miami, Miami, FL 33136, USA
Data accessibility	Repository name: Metabolomics Workbench- Project ID PR000905 Data identification number: 10.21228/M8Q69W Direct URL to data: https://www.metabolomicsworkbench.org/data/DRCCMetadata.php?Mode=Project&ProjectID=PR000905
Related research article	Tao, W., et al., *A Novel Mouse Model of Traumatic Optic Neuropathy Using External Ultrasound Energy to Achieve Focal, Indirect Optic Nerve Injury.* Sci Rep, 2017. **7**(1): p. 11779.

Value of the Data

- This data is useful for exploring metabolomic differences at the cellular level in the neurodegenerative disease process and as potential areas for further investigation in both diagnostic and therapeutic targets clinically
- This data benefits investigators studying mitochondrial changes in the settings of optic neuropathies, neuroprotection, and neuro-regeneration.
- This data will serve as a starting point for investigation into mitochondrial lipidomic as well as multi-omic approaches in the study of traumatic optic neuropathy and other neurodegenerative diseases. Additional experiments can be done to further correlate mitochondrial dysfunction with traumatic optic neuropathy, an association that is not well established in the literature.
- This data can be used to examine changes at the cellular level in other optic neuropathies and general neurodegeneration.

1. Data Description

We present here the changes that occur in the mitochondrial lipidome from the optic nerve of two-month-old C57BL/6J mice after sonication-induced TON (SI-TON) at 1, 7, and 14 days post-injury (Figure 1); time points were selected based on previous data of RGC cell loss [4, 5]. 32 mice were randomly assigned into control (uninjured, n=8) and three experimental groups (n=8 each) with even distribution of males and females (Table 1). Following SI-TON, optic nerves were harvested from all mice at their respective time points. The control group nerves were collected on day 0 (at time of sonication exposure of the other groups). Tissue was homogenized and the Mitochondrial Isolation Kit for Tissue (PIERCE, Rockford, IL, USA) was used to isolate

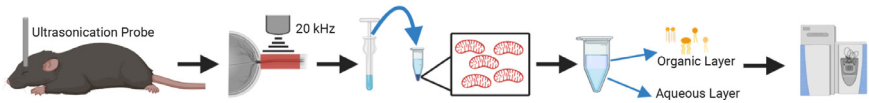

Figure 1. Schematic diagram of mitochondrial isolation and lipid extraction following sonication-induced traumatic injury. 500msec pulses were transmitted at the supraorbital rim of C57BL/6J mice. Optic nerves were harvested at three time points to assess changes following exposure. Mitochondria were isolated and their lipids were extracted. Lipids were analyzed with mass spectrometry.

Table 1
Sample Identification. 32 optic nerves with an even distribution of males and females in each group. All samples were run in positive mode and negative mode two times.

Sample	Treatment	Days Post Exposure	Sex	ESI Mode
C1	No Sonication	N/A	M	Pos + Neg
C2	No Sonication	N/A	M	Pos + Neg
C3	No Sonication	N/A	M	Pos + Neg
C4	No Sonication	N/A	M	Pos + Neg
C5	No Sonication	N/A	F	Pos + Neg
C6	No Sonication	N/A	F	Pos + Neg
C7	No Sonication	N/A	F	Pos + Neg
C8	No Sonication	N/A	F	Pos + Neg
D1_1	Sonication	1	M	Pos + Neg
D1_2	Sonication	1	M	Pos + Neg
D1_3	Sonication	1	M	Pos + Neg
D1_4	Sonication	1	M	Pos + Neg
D1_5	Sonication	1	F	Pos + Neg
D1_6	Sonication	1	F	Pos + Neg
D1_7	Sonication	1	F	Pos + Neg
D1_8	Sonication	1	F	Pos + Neg
D7_1	Sonication	7	F	Pos + Neg
D7_2	Sonication	7	F	Pos + Neg
D7_3	Sonication	7	F	Pos + Neg
D7_4	Sonication	7	F	Pos + Neg
D7_5	Sonication	7	M	Pos + Neg
D7_6	Sonication	7	M	Pos + Neg
D7_7	Sonication	7	M	Pos + Neg
D7_8	Sonication	7	M	Pos + Neg
D14_1	Sonication	14	M	Pos + Neg
D14_2	Sonication	14	M	Pos + Neg
D14_3	Sonication	14	M	Pos + Neg
D14_4	Sonication	14	M	Pos + Neg
D14_5	Sonication	14	F	Pos + Neg
D14_6	Sonication	14	F	Pos + Neg
D14_7	Sonication	14	F	Pos + Neg
D14_8	Sonication	14	F	Pos + Neg

the mitochondria. We opted for a butanol-methanol (BUME) lipid extraction instead of the gold standard Bligh and Dyer method [6] after determining that the butanol-methanol method [7, 8] extracted more lipid species as well as higher grades of lipids in the small size of our samples ($\sim$ 1 mg) (unpublished data).

We used a Q-Exactive Orbitrap Mass Spectrometer to generate the raw data for each sample. All raw data were uploaded and processed with Lipidsearch 4.1.3. We provide the lipid nomenclature in Table 2 and the identified lipids based on LipidSearch 4.1.3 in Table 3. Finally, all data were normalized and exported for bioinformatics analysis with Metaboanalyst 4.0. The lipid species heatmap (Figure 2), principal component analysis (PCA) and one-way ANOVA analysis were generated using Metaboanalyst 4.0 (Figure 3).

Table 2
LipidSearch 4.1.3 Nomenclature.

Group	Abbreviations	Lipid Name
P-	LPC	lysophosphatidylcholine
Choline	PAF	platelet-activating factor
	PC	phosphatidylcholine
	MePC	Methyl phosphatidylcholine
P-	LPE	lysophosphatidylethanolamine
Ethanol	LdMePE	lysodimethylphosphatidylethanolamine
Amine	PE	phosphatidylethanolamine
	BisMePE	Bis-methyl phosphatidylethanolamine
	dMePE	dimethylphosphatidylethanolamine
P-	LPS	lysophosphatidylserine
Serine	PS	phosphatidylserine
	BisMePS	Bis-methyl phosphatidy lserine
P-	LPG	lysophosphatidylglycerol
Glycerol	PG	phosphatidylglycerol
	BisMePG	Bis-methyl phosphatidylglycerol
P-	LPI	lysophosphatidylinositol
Inositol	PI	phosphatidylinositol
	PIP	phosphatidylinositol
	PIP2	phosphatidylinositol
	PIP3	phosphatidylinositol
P-	LPEt	lysophosphatidylethanol
Ethanol	PEt	phosphatidylethanol
P-	LPA	lysophosphatidic acid
Acid	BisMeLPA	Bis-methyl lysophosphatidic acid
	PA	phosphatidic acid
	BisMePA	Bis-methyl phosphatidic acid
	cPA	cyclic phosphatidic acid
P-	LPMe	Lysophosphatidylmethanol
Methanol	PMe	phosphatidylmethanol
Sphingolipids	SM	sphingomyelin
	LSM	lysosphingomyelin
	phSM	sphingomyelin(phytosphingosine)
Neutral	MG	monoglyceride
glycerolipid	DG	diglyceride
	TG	triglyceride
Fatty Acid	FA	fatty acid
Cardiolipin	CL	Cardiolipin
Sphingoid	So	Sphingosine
base	SoP	Sphingosine phosphate
Neutral	SoG1	Glucosylsphingosine
Glycosphingolipids	CerG1	Simple Glc series
	CerG2	Simple Glc series
	CerG3	Simple Glc series
	CerG2GNAc1	Simple Glc series
	CerG3GNAc1	Simple Glc series
	CerG3GNAc2 ST	Simple Glc series Sulfatide
Glycosphingolipids	Cer	Ceramides
	CerP	Ceramides phosphate
	GM3	Gangliosides
	GM2	Gangliosides
	GM1	Gangliosides
	GD1a	Gangliosides
	GD1b	Gangliosides
	GD2	Gangliosides
	GD3	Gangliosides
	GT1a	Gangliosides
	GT1b	Gangliosides
	GT1c	Gangliosides
	GT2	Gangliosides
	GT3	Gangliosides
	GQ1c	Gangliosides
	GQ1b	Gangliosides

(*continued on next page*)

Table 2 (*continued*)

Group	Abbreviations	Lipid Name
Steroid	ChE	Cholesterol Ester
	ZyE	Zymosterol
	StE	Stigmasterol ester
	SiE	Sitosterol ester
	AGlcSiE	AcylGlcSitosterol ester
	D7ChE	Deuterated Cholesterol Ester
Coenzyme	Co	Coenzyme
Fatty	OAHFA	(O-acyl)-1-hydroxy fatty acid
Ester	WE	wax exters
	AcCa	Acyl Carnitine
Glycoglycerolipid	MGMG	Monogalactosylmonoacylglycerol
	MGDG	Monogalactosyldiacylglycerol
	DGMG	Digalactosylmonoacylglycerol
	DGDG	Digalactosyldiacylglycerol
	SQMG	Sulfoquinovosylmonoacylglycerol
	SQDG	Sulfoquinovosyldiacylglycerol
Neutral glycerolipid (deuterat	D5DG	Deuterated diglyceride
	D5TG	Deuterated triglyceride

Table 3
Identified LipidSearch 4.1.3 Lipids. All lipids as identified with base retention times and calculated masses displayed.

Lipid Class	Lipid Species	Calculated Mass	Formula	Base Retention Time
BisMePA	BisMePA(18:2p/20:1)	738.5563	C43 H79 O7 N0 P1	14.204
CerG1	CerG1(d18:0+pO/22:1)	799.6537	C46 H89 O9 N1	14.055
	CerG1(d18:0+pO/24:1)	827.685	C48 H93 O9 N1	14.356
	CerG1(d18:1/22:0+O)	799.6537	C46 H89 O9 N1	13.382
	CerG1(d18:1/22:1)	781.6432	C46 H87 O8 N1	13.39
	CerG1(d18:1/24:1)	809.6745	C48 H91 O8 N1	14.391
	CerG1(d18:1/24:2)	807.6588	C48 H89 O8 N1	13.457
	CerG1(d40:0+pO+O)	817.6643	C46 H91 O10 N1	13.378
	CerG1(d42:1+pO)	827.685	C48 H93 O9 N1	13.892
LPC	LPC(16:0)	495.3325	C24 H50 O7 N1 P1	4.906
	LPC(18:0)	523.3638	C26 H54 O7 N1 P1	6.07
	LPC(18:1)	521.3481	C26 H52 O7 N1 P1	5.281
	LPC(18:2)	519.3325	C26 H50 O7 N1 P1	4.625
	LPC(20:4)	543.3325	C28 H50 O7 N1 P1	4.791
PA	PA(16:0/18:1)	674.4887	C37 H71 O8 N0 P1	34.197
	PA(18:0/18:1)	702.52	C39 H75 O8 N0 P1	35.43
PC	PC(16:0/18:1)	759.5778	C42 H82 O8 N1 P1	33.78
	PC(18:0/18:1)	787.6091	C44 H86 O8 N1 P1	34.914
	PC(32:0)	733.5622	C40 H80 O8 N1 P1	12.275
	PC(34:1)	759.5778	C42 H82 O8 N1 P1	12.665
	PC(36:1)	787.6091	C44 H86 O8 N1 P1	13.996
PE	PE(18:0/18:1)	745.5622	C41 H80 O8 N1 P1	14.41
	PE(18:0p/18:1)	729.5672	C41 H80 O7 N1 P1	14.078
	PE(18:0p/20:1)	757.5985	C43 H84 O7 N1 P1	14.93
	PE(18:1p/18:1)	727.5516	C41 H78 O7 N1 P1	13.052
PEt	PEt(16:0/18:1)	702.52	C39 H75 O8 N0 P1	35.43
PS	PS(18:0/18:1)	789.552	C42 H80 O10 N1 P1	14.155
	PS(18:0/20:1)	817.5833	C44 H84 O10 N1 P1	14.981
SM	SM(d42:2)	812.6771	C47 H93 O6 N2 P1	13.849
TG	TG(16:0/16:0/18:1)	832.752	C53 H100 O6	13.847
	TG(16:0/18:1/18:1)	858.7676	C55 H102 O6	14.736
	TG(16:0/18:1/18:2)	856.752	C55 H100 O6	14.254
	TG(18:0/16:0/18:1)	860.7833	C55 H104 O6	15.378
	TG(18:1/18:1/18:1)	884.7833	C57 H104 O6	15.135
	TG(18:1/18:1/18:2)	882.7676	C57 H102 O6	14.778
	TG(18:1/18:2/18:2)	880.752	C57 H100 O6	15.476
dMePE	dMePE(34:2p)	727.5516	C41 H78 O7 N1 P1	34.147

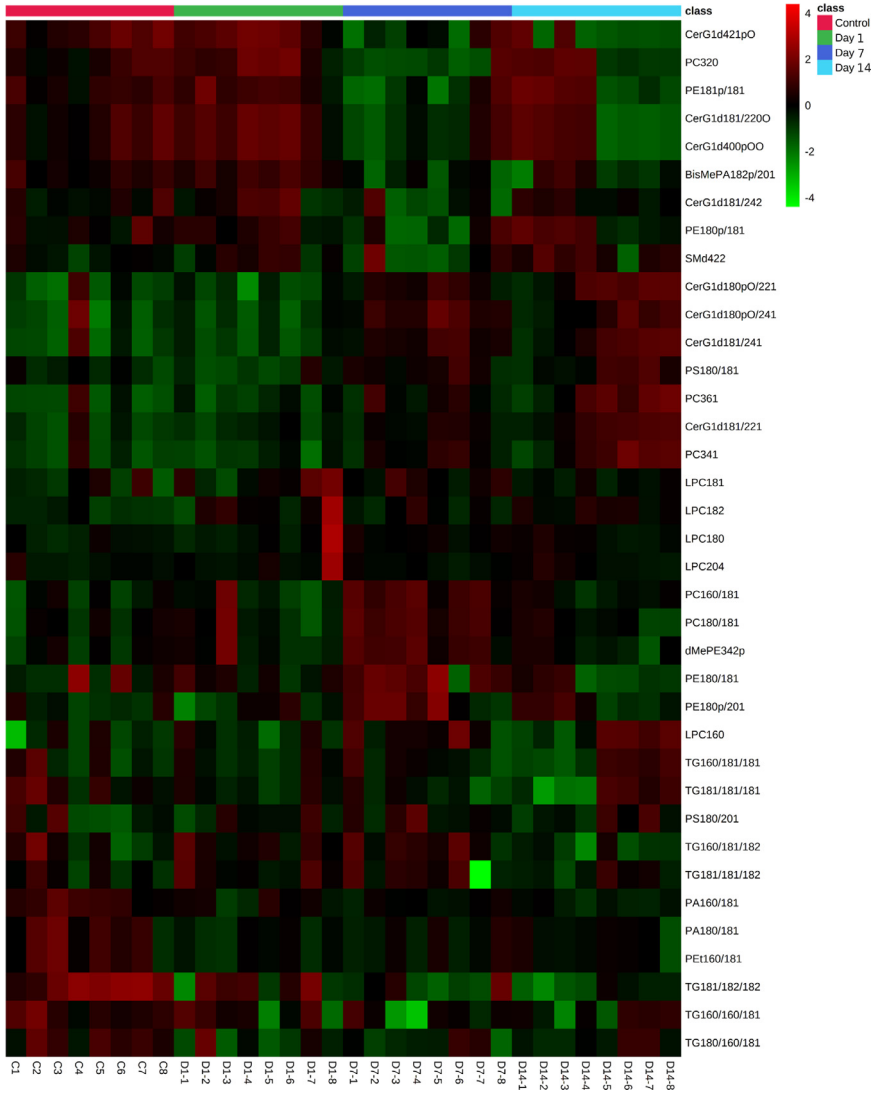

Figure 2. Heat map of mitochondrial lipid species. Lipid species changes depicted at control (uninjured), 1-day, 7-days, and 14-days post-sonication.

2. Experimental Design, Materials, and Methods

2.1. Animals

Animals were treated in accordance with the National Research Council's Guide for the Care and Use of Laboratory Animals and the Association for Research in Vision and Ophthalmology (ARVO) Statement for the Use of Animals in Ophthalmic and Vision Research. All procedures involving mice were approved by the Institutional Animal Care and Use Committee (IACUC) at the University of Miami. C57BL/6J mice from Jackson Laboratory (Bar Harbor, ME, USA) were

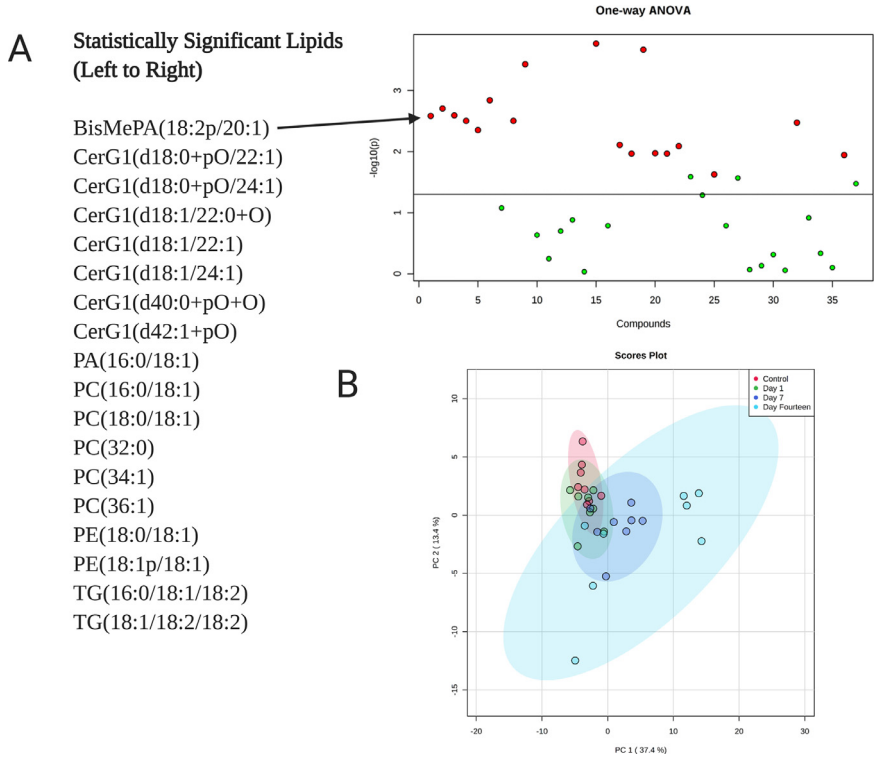

Figure 3. One-Way Analysis of Variance and Principal Component Analysis. A. ANOVA displayed 18 statistically significant lipids out of 37 lipids identified. Only statistically significant lipids listed (in order from left to right). B. PCA with 95% confidence intervals

maintained in a temperature-regulated environment with a 12-hour light, 12-hour dark cycle. All mice were fed ad libitum. Two-month-old mice were used.

2.2. Sonication-Induced Traumatic Optic Neuropathy (SI-TON) Model

SI-TON was performed as described previously [4]. TON was induced in C57BL/6J mice with a Branson Digital Sonifier 450 (Branson Ultrasonics, Danbury, CT, USA) by a 3mm microtip probe in a soundproof chamber. Mice were anesthetized with vaporized isoflurane supplied with oxygen. Supraorbital fur was shaved, and the microtip probe was placed directly above the insertion point of the optic nerve into the optic canal. Left optic nerves were injured with a 500 msec shock at a 35% amplitude providing 20 kHz ultrasound waves. Following sonication, mice were placed in a new cage with thermal support until fully recovered.

2.3. Sample Preparation and Mitochondrial Isolation

Optic nerve samples were collected at 1 day, 7 days, and 14 days post-sonication. The mice brain was carefully removed to expose the underlying optic nerves and tracts. Optic nerves were harvested starting at the optic nerve head and dissecting at the optic chiasm. Optic nerves were dried and weighed to approximately 1 mg. Mitochondria were isolated using the Mitochondrial Isolation Kit for Tissue (PIERCE, Rockford, IL, USA). The protocol was modified for use in our

small samples. Briefly, optic nerves were washed twice in 1x Phosphate Buffered Saline (PBS) to remove all fat and debris. Samples were then resuspended in 200 µl of BupH PBS and carefully dounced 15 times. Homogenate was centrifuged at 1,000 x g at 4°C for 3 minutes and supernatant was discarded. The pellet was resuspended in 200µl of Reagent A and vortexed at maximum speed for 5 seconds. Samples were then incubated for 2 minutes on ice. 2.5 µl of Reagent B were added and incubated on ice for 5 minutes with 5 seconds of vortexing at every minute of incubation. 200 µl of Reagent C were added, the tube was inverted for mixing, and then centrifuged at 700 x g for 10 minutes. The pellet was discarded and supernatant was again centrifuged at 3,000 x g for 15 minutes. This resultant mitochondrial pellet was kept and supernatant was stored for cytosolic analysis. The mitochondrial pellet was washed with wash buffer and placed on ice for subsequent lipid extraction. Mitochondrial isolation was validated by dot blot targeting for TOM20, a mitochondrial membrane protein.

2.4. Butanol-Methanol (BUME)Lipid Extraction

Lipids were extracted using a modified BUME lipid extraction as performed by Cruz and Lofgren [7, 8]. Briefly, mitochondrial pellets were resuspended in 300 µl n-butanol: methanol 3:1 (v/v) and vortexed for one minute. 150 µl of heptane: ethyl acetate 3:1 (v/v) was then added to the test tube and vortexed for one minute followed by another 150 µl of heptane/ ethyl Acetate 3:1 (v/v) and another minute of vortexing. Phase separation was induced by adding 300 µl of 50 mM LiCl followed by vortexing for one minute. Here, with two layers visible, the samples were centrifuged at 2,700 x g for 10 minutes. The upper layer (organic) was collected and the bottom layer (aqueous) was re-extracted by phase separation two more times. The organic layers were combined and dried using a SpeedVac Concentrator. Samples were stored dry in -80°C for further processing. A bicinchoninic acid (BCA) protein assay was performed on the aqueous protein layer to normalize the lipid concentrations in each sample using the Pierce Micro BCA Protein Assay Kit (PIERCE, Rockford, IL, USA).

2.5. High Performance Liquid Chromatography and Mass Spectrometry

Lipid samples were resuspended in 50µl of chloroform: methanol 2:1 (v/v), placed in an ultrasonic water bath for 20 minutes, and then vortexed for 2 minutes. 30 µl were loaded into vials for four runs (two positive, two negative) of 5 µl each. Lipids were analyzed with liquid chromatography electrospray tandem mass spectrometry (LC-MS/ MS) using the Accela HPLC system and an orbitrap mass spectrometer (Q-Exactive, Thermo Scientific, Waltham, MA). An Acclaim 120 C18 3µm column (Thermo Scientific) was used with LC-MS grade methanol: water 60:40 (v/v) with 10mM ammonium acetate and methanol chloroform 60:40 (v/v) with 10mM ammonium acetate, as solvent A and B, respectively. A Heated Electrospray Ionization Source (HESI) was operated at a spray voltage of 4,415 V, a HESI vaporization temperature of 275°C, and an auxiliary gas flow of 15 arbitrary units. The scan range was set at 150-1500 m/z. The gradient ran at 35% to 100% Solvent B for 13 minutes, held at 35% solvent B for 2 minutes and finally brought up to 100% solvent A for 3 minutes and held for 2 minutes. The LC-MS/ MS method was validated for mitochondrial lipid analysis using external standards with known concentrations of cardiolipin.

2.6. Lipid Identification and Bioinformatics Analysis

Raw data produced by LC-MS/MS was uploaded to LipidSearch 4.1.3. The parameters were set to an M-score of 5.0, Productsearch, precursor (5/5) ppm, intensity threshold of 1.0% and quantitation and TopRank filter were turned on. ID quality were graded from A-D. All target classes

were selected. All adducts for both negative and positive modes were selected with the exception of (CH3CH2)3NH+ and (CH3)2NH2. Once all peaks were identified, samples were aligned in positive mode, negative mode, and also all trial runs in one. Lipid identification was graded from A-C with an M-Score of 5. Any false positive peaks were rejected. All aligned data was exported and formatted for further analysis in Metaboanalyst 4.0. The data was normalized by pooling the control group, log transforming, scaling by mean-centering and dividing by the square root of the standard deviation (pareto scaling). A heat map (Figure 2) was generated along with PCA and one-way ANOVA (Figure 3) analyses. 18 of the 37 lipids were statistically significant (p-value set to 0.05).

Declaration of Competing Interest

The authors declare that they have no known competing financial interests or personal relationships which have, or could be perceived to have, influenced the work reported in this article.

Acknowledgments

This work was supported in part by NIH grant U01EY027257, NIH Center Core Grant P30EY014801, an unrestricted grant from Research to Prevent Blindness to Bascom Palmer Eye Institute, and the Dr. Al-Rashid Orbital Research Center Endowment. Metabolomics workbench is an effort of NIH Common Fund's Metabolomics Data Repository and Coordinating Center supported by U2C DK119886.

References

[1] A.M. Kumaran, G. Sundar, L.T. Chye, Traumatic optic neuropathy: a review, Craniomaxillofac Trauma Reconstr 8 (1) (2015) 31–41.
[2] V. Carelli, et al., Optic neuropathies: the tip of the neurodegeneration iceberg, Hum Mol Genet 26 (R2) (2017) R139–r150.
[3] Y.L. Pilz, S.J. Bass, J. Sherman, A Review of Mitochondrial Optic Neuropathies: From Inherited to Acquired Forms, J Optom 10 (4) (2017) 205–214.
[4] W. Tao, et al., A Novel Mouse Model of Traumatic Optic Neuropathy Using External Ultrasound Energy to Achieve Focal, Indirect Optic Nerve Injury, Sci Rep 7 (1) (2017) 11779.
[5] R. Nuesi, et al., Lipidomics dataset of sonication-induced traumatic optic neuropathy in mice, Data Brief 29 (2020) 105147.
[6] E.G. Bligh, W.J. Dyer, A rapid method of total lipid extraction and purification, Can J Biochem Physiol 37 (8) (1959) 911–917.
[7] M. Cruz, et al., Improved Butanol-Methanol (BUME) Method by Replacing Acetic Acid for Lipid Extraction of Biological Samples, Lipids 51 (7) (2016) 887–896.
[8] L. Lofgren, et al., The BUME method: a novel automated chloroform-free 96-well total lipid extraction method for blood plasma, J Lipid Res 53 (8) (2012) 1690–1700.